Molecular Simulation and Experimental Study of Substituted Polyacetylenes: Fractional Free Volume, Cavity Size Distributions and Diffusion Coefficients

Xiao-Yan Wang, Roy D. Raharjo, Hyuck J. Lee,[†] Ying Lu, B. D. Freeman, and I. C. Sanchez*

Department of Chemical Engineering, University of Texas at Austin, Austin, Texas 78712

Received: January 12, 2006; In Final Form: April 21, 2006

Glassy, disubstituted acetylene-based polymers exhibit extremely high gas permeabilities and high vapor/gas selectivities, which is quite unusual for conventional glassy polymers such as polysulfone. Diffusion coefficients of poly[1-phenyl-2-[*p*-(trimethylsilyl)phenyl]acetylene] (PTMSDPA) and poly[diphenylacetylene] (PDPA) were obtained using both molecular simulation and experimental techniques. PTMSDPA, a disubstituted glassy acetylene-based polymer, exhibits higher diffusivity than its desilylated analogue, PDPA. Simulation results are in good agreement with experimental data. Cavity size (free volume) distributions of both polymers are also obtained using an energetic-based algorithm (in't Veld et al., *J. Phys. Chem. B* **2000**, *104*, 12028) developed recently. Larger cavities in PTMSDPA contribute to its higher diffusivity, and higher permeability.

1. Introduction
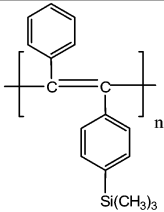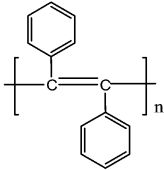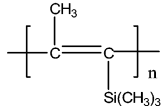
There is a growing interest in the substituted polyacetylenes following the synthetic work of Masuda and Higashimura.[1,2] The substituted polyacetylenes show very high gas permeabilities and vapor/gas selectivities, which is unusual for conventional glassy polymers such as polysulfones.[3] They are more permeable to larger and more soluble organic vapors than to smaller, less soluble permanent gases.[3]

The first substituted acetylene-based polymer, poly(1-trimethylsilyl-1-propyne) (PTMSP), has very high fractional free volume and the highest gas permeabilities among all known polymers.[1,4] Mixed-gas selectivities of organic vapors over permanent gases for PTMSP are 27 for $n\text{-}C_4H_{10}/CH_4$ and 39 for $n\text{-}C_4H_{10}/H_2$, which represents the highest performance for these separations among all polymers.[5] Such high vapor/gas selectivity could have potential application in organic vapor separation processes.

However, several issues prevent PTMSP's commercial practice. One issue is PTMSP's lack of chemical resistance. PTMSP is soluble in many organic compounds such as toluene and hexane. Another issue is PTMSP's physical aging.[6] The gas permeabilities of PTMSP decrease with time. The drawbacks of PTMSP have motivated researchers to explore new substituted polyacetylenes to improve physical aging and chemical resistance.

Poly[1-phenyl-2-[*p*-(trimethylsilyl)phenyl]acetylene] (PTMSDPA) and poly[diphenylacetylene] (PDPA) are two recently synthesized substituted acetylene-based polymers. PTMSDPA is also a highly permeable and vapor selective polymer.[7,8] PTMSDPA has a fractional free volume (FFV) of 0.24, and it is more permeable to larger and more condensable hydrocarbons than to smaller and less condensable permanent gases.[7,8] Unfortunately, PTMSDPA also exhibits poor chemical resistance. PTMSDPA, like PTMSP, is soluble in common organic

TABLE 1: Physical Properties of Substituted Polyacetylenes

Polymer	Chemical Structure	Density g/cm³	FFV[a]
PTMSDPA		0.91	0.24
PDPA		1.04	0.19
PTMSP		0.75	0.34

[a] FFV, fractional free volume which is obtained using the Bondi group contribution method.

solvents. PDPA is synthesized by removing the trimethylsilyl (TMS) group from PTMSDPA (desilylation).[7,8] PDPA is thermally stable and completely insoluble in any organic solvent. Table 1 presents some properties and the chemical structures of PTMSDPA and PDPA along with those of PTMSP.

It is of great interest to understand the influence of desilylation on free volume, cavity size (free volume) distribution and also transport properties of small molecules in PTMSDPA. In this work, the free volume, cavity size distributions of PTMSDPA and PDPA will be characterized using the molecular simulation technique. Diffusion coefficients of CO_2 in the two polymers obtained using both molecular simulation and experimental methods will be compared.

* Corresponding author phone: (512)-471-1020. E-mail: Sanchez@che.utexas.edu.
† Current address: Department of Technology Information Analysis, Korea Institute of Science and Technology Information, 206−9, Cheong-nyangni-dong, Dongdaemun-gu, Seoul, Korea 130-742.

Simulation and Experimental Study of Polyacetylenes

J. Phys. Chem. B, Vol. 110, No. 25, 2006 **12667**

Cavity size distribution can be estimated experimentally using positron annihilation lifetime spectroscopy (PALS) experiments[9] and photochromic labeling.[10] PALS can measure the size and concentration of static and dynamic free volume elements in condensed matter.[9] However, the cavity size distribution of a material is not easy to access experimentally. Molecular modeling provides an alternative way to determine the cavity size distribution of materials. The most widely used method is Delaunay and Voronoi tessellation,[11,12] which is a geometric approach. In this method, the entire three-dimensional space is subdivided into tetrahedra, and the vertices of the fundamental space elements coincide with atom centers, which describes the unoccupied volume composed by the cavities. In this work, we will apply an algorithm[13] recently developed in our group (the so-called cavity energetic sizing algorithm (CESA)) to study the cavity size distributions of PTMSDPA and PDPA. In the CESA algorithm, the cavity is defined as a spherical volume with a well-defined center, and that center as a local minimum in a repulsive particle energy field. Basically, the CESA algorithm is based on energetic rather than geometric considerations. It has been employed successfully to describe both liquid structure and polymer structures.[13−16]

To examine the effect of desilylation on PTMSDPA, the cavity size distributions of PTMSDPA and PDPA were calculated using CESA algorithm. Additionally, the CO_2 diffusivity, solubility, and permeability in PTMSDPA were calculated by molecular simulation. For comparison, the solubility and permeability of CO_2 in these two polymers were also measured experimentally.

2. Methodology

2.1. Permeability. The steady-state gas permeability coefficient of a polymer film is defined by the following relationship:[17,18]

$$P = \frac{Nl}{p_2 - p_1} \tag{1}$$

where P is the gas permeability coefficient (cm^3(STP)·cm/(cm^2·s·cmHg)), N is the steady-state penetrant flux (cm^3(STP)/(cm^2·s)), l is the film thickness (cm), and p_1 and p_2 are the downstream (permeate) and upstream (feed) pressure (cmHg), respectively. The permeability is often expressed in Barrers, and 1 Barrer = $10^{-10}cm^3$(STP)·cm/(cm^2·s·cmHg), where STP represents standard temperature (273.15 K) and pressure (1 atm).

When Fick's law is obeyed, and the downstream pressure is much less than the upstream pressure, the permeability coefficient defined in eq 1 can also be expressed as a product of diffusivity and solubility:

$$P = SD \tag{2}$$

where S is the solubility coefficient, and D is an average diffusion coefficient. Permeability is often measured experimentally by the constant pressure/variable volume method. In this study, we will calculate the diffusivity and solubility of CO_2 in PTMSDPA through molecular modeling. Then, we will obtain the permeability of CO_2 in PTMSDPA based on eq 2. We will also measure permeability and solubility of CO_2 in PTMSDPA and PDPA experimentally, and then get the diffusivity based on eq 2.

2.2. Solubility. Experimentally, the sorption[18] of penetrants into a glassy polymer is usually described by the dual mode model:

$$C = k_D p + \frac{C'_H bp}{1 + bp} \tag{3}$$

where C is the equilibrium penetrant concentration in the polymer at pressure p(atm); it has units of (volume of penetrant (cm^3)/volume of polymer (cm^3)). k_D is the Henry's law parameter which describes penetrant dissolution into the equilibrium densified polymer matrix. C'_H is the Langmuir capacity of the glassy polymer, and b is the Langmuir affinity parameter describing the affinity of a penetrant for a Langmuir site. The Langmuir capacity is equivalent to the maximum concentration of solute molecules in the unrelaxed (Langmuir) matrix of a glassy polymer. It can be viewed as a measure of excess free volume in a polymer.

The solubility of a penetrant in a polymer is defined as the ratio of equilibrium penetrant concentration to penetrant pressure:[18]

$$S = \frac{C}{p} = k_D + C'_H \frac{b}{1 + bp} \tag{4}$$

The infinite dilute solubility coefficient, S_0, is calculated as follows:

$$S_0 \equiv \lim_{p \to 0} \frac{C}{p} = k_D + C'_H b \tag{5}$$

S_0, also called the Henry's law solubility coefficient, can be calculated using the Widom insertion method[19] through molecular simulation. In this method, we calculate the energy Δu of randomly inserting a particle into a molecular configuration. Δu is the interaction energy between the inserted particle and the rest of the particles in the system. The dimensionless solubility, also called Widom insertion factor B, is defined as

$$B = \langle \exp(-\Delta u/kT) \rangle \tag{6}$$

where $\langle \Lambda \rangle$ represents an ensemble average. The Widom insertion method is most effective for systems with high fractional free volume systems. For low free volume systems, most of the inserted molecules have such a high energy that the Boltzmann factor in eq 6 is negligible. Once in a while, a hole in the polymer structure is found that provides a nonzero contribution to this Boltzmann factor. However, the statistical accuracy is very low with these rarely observed nonzero contributions.[19] The dimensionless insertion factor B is related to the experimentally determined solubility coefficient S_0 as follows:[20−22]

$$B = \frac{T}{273.15} S_0 = \frac{T}{273.15} (k_D + C'_H b)(1 \text{ atm}) \tag{7}$$

2.3. Diffusion. Experimentally, diffusion coefficients are usually calculated from permeability and solubility data using eq 2. Permeability and solubility can be measured as described in the Experimental Section of this manuscript.

In molecular simulation, diffusion coefficients are calculated from the Einstein relationship:[19]

$$D_i = \lim_{t \to \infty} \frac{1}{6t} \langle [\mathbf{r}_i(t) - \mathbf{r}_i(0)]^2 \rangle \tag{8}$$

where $\mathbf{r}_i$ is the position vector of atom i, ·$[\mathbf{r}_i(t) - \mathbf{r}_i(0)]^2 \rangle$ represents the ensemble average of the mean-square displacement of the inserted gas molecule trajectories; $\mathbf{r}_i(t)$ and $\mathbf{r}_i(0)$ are the final and initial positions of the center of mass of the

gas molecules over the time interval t. The diffusion coefficient can also be calculated from the velocity autocorrelation function.[19]

3. Model and Simulation Details

3.1. **Building Amorphous Cells.** The Materials Studio[23] software package of Accelrys Inc. was used to construct the amorphous packing structure. The COMPASS force field[24] was used in all simulations, and it models each molecule in an atomistic way. The nonbonded interactions of the COMPASS force field include a Lennard−Jones 9−6 function for the van der Waals interaction and a Coulombic function for the electrostatic interaction. The amorphous cell module of Materials Studio constructs the initial structure of polymers, which is capable of folding a polymer onto itself at all densities by using its mirror images.

Two PTMSDPA chains (each with 50 repeat units) were folded in the amorphous cell at a density of 0.91 g/cm³, which corresponds to the experimental density. The resulting cell length was 29.2 Å. 50 initial states were constructed and followed by 5000 steps of energy minimization to eliminate "hot spots". Afterward, a 10 ps NVT MD run at 298 K was performed for each of the 50 states to equilibrate structures. The smart minimizer method which combines the steepest descent, conjugate gradient and newton methods in a cascading manner was used to minimize the energy of the molecular structure. The convergence level was set to 0.1 kcal/mol/Å. The smart minimizer is part of the amorphous cell module.

For PDPA, the initial polymer chain was constructed from 50 repeat units with a density of 1.04 g/cm³, which corresponds to the experimental density. The resulting cell length was around 24.3 Å. 50 initial states were constructed and followed by 10 000 energy minimization steps and a 10 ps MD run in the NVT ensemble. The temperature was also set to 298 K.

It is assumed that the resulting equilibrated structures are representative of the glassy polymers.

3.2. **Simulation of Cavity Size Distribution.** The CESA was applied to each of the above equilibrated structures. The description below provides a brief review of CESA:

(i) A polymer structure is created by MD (or MC) simulation.

(ii) The force field used to generate the structure from step i is replaced with a pure repulsive force field. All atoms remain in fixed positions.

(iii) A trial repulsive particle is then randomly inserted into the repulsive structure, and a local energy minimum is located in the repulsive force field by the multivariable Newton method combined with the steepest descent method.

(iv) After the minimum is determined, attractive interactions are turned on, and the size of the test particle is adjusted until its potential interaction with all other atoms becomes zero. This size is taken as the diameter of a spherical cavity.

(v) A check is then made to determine whether the initial random insertion point is inside the cavity or not. The cavity is only accepted if the initial point is inside the cavity. This procedure leads to a volume distribution rather than a number distribution of cavities.

(vi) Steps iii−v are repeated many times to produce a representative distribution of cavity sizes for a given structure.

3.3. Simulation of Diffusion, Solubility and Permeability Coefficients. Diffusion coefficients were determined by adding five CO_2 molecules to each of 10 independent states. After each state was equilibrated for 10 ps, the diffusion constants were calculated by molecular center of mass displacement over a 200 ps interval for PTMSDPA and a 100 ps interval for PDPA.
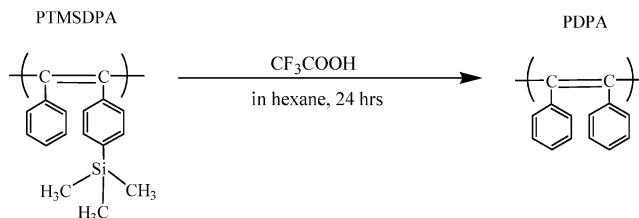

Figure 1. Desilylation Reaction.

Finally, an average value of D was calculated from 10 independent states. Charati and Stern[25] have calculated diffusion coefficients of He, O_2, N_2, CH_4, and CO_2 in four silicone polymers by means of the Einstein equation with a simulation time of 200 ps. Their plots of mean square displacements (MSD) versus time are linear for all penetrant gases over a period time of about 100 ps, and all estimated diffusion coefficients, D, were determined from the linear parts of the plots. Our group[15] also simulated the diffusion coefficient of CO_2 in PTMSP with a simulation time of 100 ps, and good agreement is obtained between the simulation and experiment.

The Widom insertion method[19] was used to simulate the solubility of CO_2 in PTMSDPA. For PTMSDPA's 50 configurations, we performed 20 000 CO_2 configurations.

The permeability coefficient is then obtained using eq 2.

4. Experimental Section

4.1. Polymer Film Preparation. Films of PTMSDPA were prepared from a 1 wt % solution of the polymer in toluene. The solution was filtered through filter paper using a syringe and then cast into a Petri dish. After drying at ambient conditions for 3−5 days, the samples were stored in liquid methanol until the day before use to prevent physical aging. Prior to permeation experiments, samples were removed from methanol and dried at ambient conditions for approximately 15 h. The film thickness of these samples was approximately 73 μm.

PDPA was synthesized from PTMSDPA samples following the desilylation procedure reported in the literature.[7] A PTMSDPA film (0.118 g) was placed in a 50 mL mixture of trifluoroacetic acid and *n*-hexane (50/50 by volume) at ambient conditions for approximately 24 h. Trifluoroacetic acid removes the trimethylsilyl groups from PTMSDPA (see Figure 1), while *n*-hexane serves as a diluent. The samples were then washed with *n*-hexane and immersed in a mixture of triethylamine and *n*-hexane (50/50 by volume) for 24 h to neutralize any remaining trifluoroacetic acid. The films were rinsed with *n*-hexane and stored in methanol for at least 24 h before being used. Prior to permeation experiments, PDPA samples were removed from methanol and dried at ambient conditions for approximately 15 h. The final thickness of PDPA films for permeation measurements was approximately 62 μm.

FT−IR spectra of the samples before and after reaction were acquired using a Nexus 470 FT−IR spectrometer from Thermo Nicolet (Madison, WI). After desilylation, the spectrum shows no absorption at 1248 (δ_s Si−CH), 1116, 856 (ν_{as} Si−CH3), and 811 (ν_s Si−CH3) cm⁻¹, indicating that the desilylation was complete[7,8] (see Figure 2).

4.2. Permeation Measurements. The permeability of PTMSDPA and PDPA films to CO_2 at 35 °C was determined using the constant-pressure/variable volume method.[26] The permeate gas flow rate was measured with a soap film flowmeter. The upstream pressure was set at 4.46 bar, and the downstream pressure was at atmospheric. Each sample took 8 hours.[8] The films did not show any aging effects during the course of the permeability measurements.
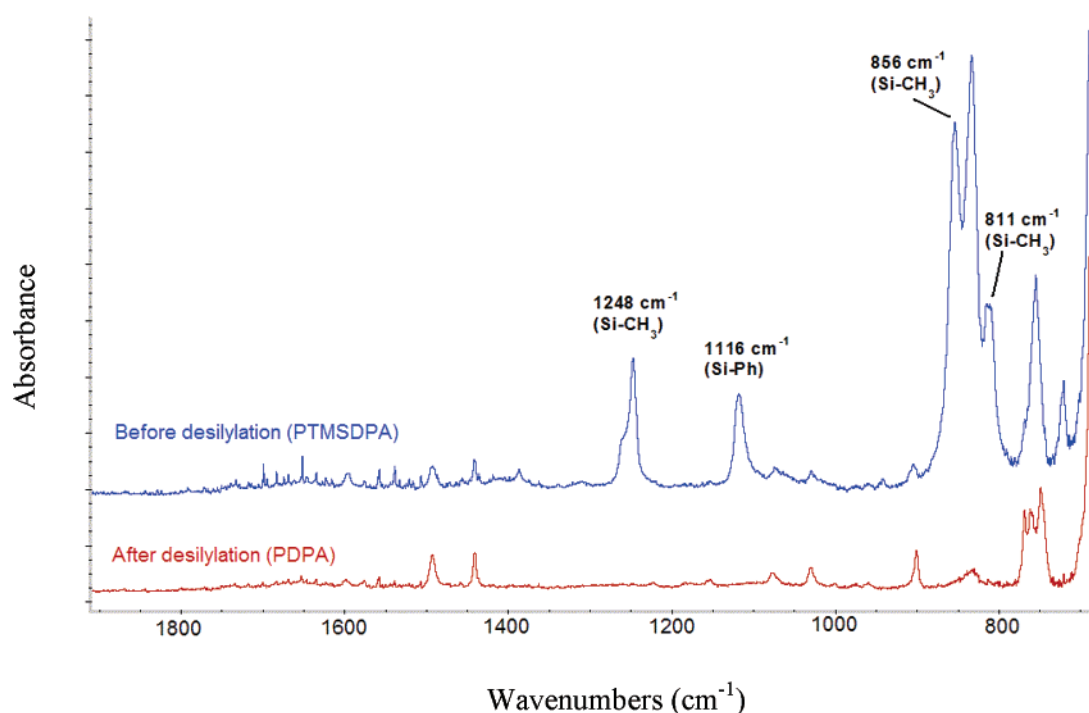
Figure 2. FT−IR spectrum of PTMSDPA and PDPA.

The gas permeability coefficient P (cm^3(STP)·cm/(cm^2·s·cmHg)) was calculated using the following expression:

$$P = \frac{l}{\Delta p} \frac{273}{TA} \frac{P_{atm}}{76}\left(\frac{dV}{dt}\right) \qquad (9)$$

where Δp is the difference between the upstream and downstream pressures (i.e., $p_2 - p_1$) (cmHg), p_{atm} is the atmospheric pressure (cmHg), A is the membrane area (cm^2), T is temperature (K), l is the membrane thickness (cm), and dV/dt is the volumetric displacement rate of the soap film in the bubble flowmeter at steady state.

4.3. Solubility Measurements. The solubility of CO_2 in the polymer was measured with a high-pressure, barometric sorption apparatus.[27] Initially, a polymer film was placed in the sample chamber and exposed to vacuum overnight to remove air gases. A known amount of penetrant gas was introduced into the chamber, and the pressure was allowed to equilibrate. The amount of gas sorbed in the polymer can be determined by mass balance calculations.[26] Once the chamber pressure was constant, additional penetrant was introduced, and the procedure was repeated. In this incremental manner, penetrant uptake as a function of pressure was determined. The maximum penetrant pressure was 18 atm. The system temperature was maintained at 35°C ($\pm$ 0.1°C) using a constant-temperature bath.

The diffusion coefficient is then obtained using eq 2.

5. Results and Discussion

5.1. Fractional Free Volume (FFV), and Fractional Cavity Volume (FCV). Figure 3 shows a typical structure of PTMS-DPA from molecular dynamics simulation. Table 2 presents the fractional free volume (FFV), the fractional cavity volume (FCV) and the average cavity size of PTMSDPA, PDPA, and PTMSP. PTMSP has the highest permeability among all known glassy polymers. All these polymers have rigid polyacetylene backbones and two bulky substituents attached to the backbone, which may contribute to inefficient chain packing and, in turn,
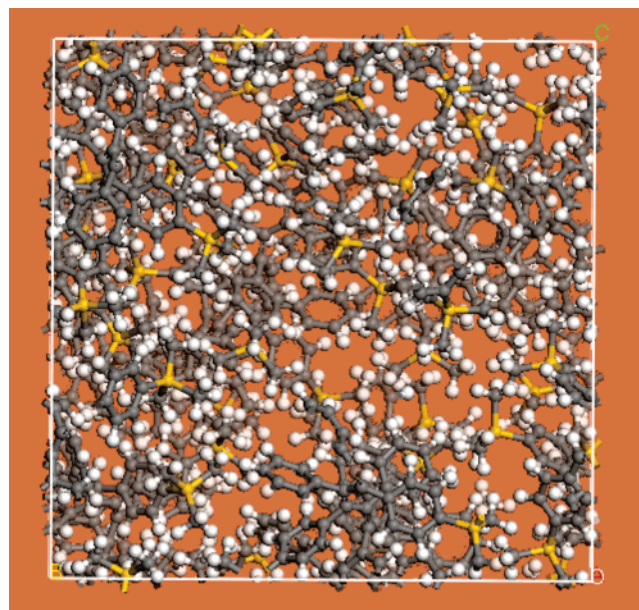

Figure 3. A typical packing structure for PTMSDPA. Large cavities are observed.

TABLE 2: Comparison of Fractional Free Volume (From the Bondi Method[28]), Fractional Cavity Volume, Average Cavity Size, and Permeability of PTMSP, PTMSDPA, and PDPA

polymer	FFV%	FCV%	average cavity size (Å)	$P(O_2)$ (barrer)
PTMSP	34	15.6 $\pm$ 1.8	11.2	9700
PTMSDPA	24	12.3 $\pm$ 0.7	7.5	1200
PDPA	19	10.8 $\pm$ 0.5	5.0	490

high free volume and high permeability. These polymers are all more permeable to large, condensable vapors (e.g., *n*-butane) than to small, permanent gases (e.g., methane).[8] The FFV is commonly used to characterize the efficiency of chain packing
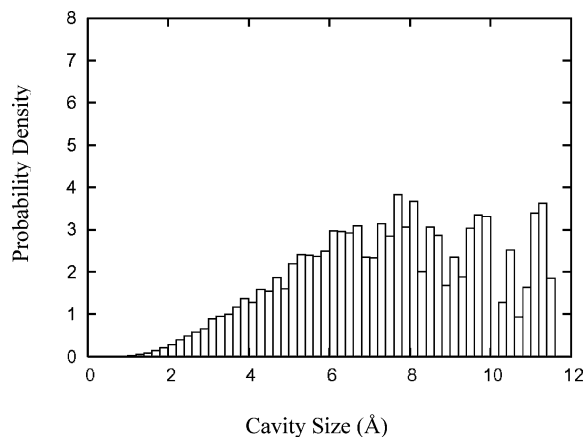
12670 *J. Phys. Chem. B, Vol. 110, No. 25, 2006*

Wang et al.

Figure 4. Cavity size distribution in PTMSDPA at $T = 298$ K and $\rho = 0.91$ g/cm^3 from molecular simulation. The average cavity size is 7.5 Å, and the fractional cavity volume is 12.3%. PTMSDPA has much higher permeability than PDPA (see Table 2). PTMSDPA has a smaller fraction of smaller cavities than PDPA (see Figure 5).

and the amount of free space in a polymer matrix. A common definition of FFV is

$$FFV = \frac{v - v^*}{v} \qquad (10)$$

where v is the specific volume. Usually, v^*, the so-called occupied volume, is determined from tabulated van der Waals' volumes (v_w) and the Bondi recipe $v^* = 1.3v_w$.[28] The FFV values presented in Table 2 are determined using this method.[28] These polymers have greater free volume than conventional glassy polymers such as poly(methyl acrylate) (PMA), which has a FFV value of 0.20 by the Bondi method and 0.18 from zero pressure PVT data.[29]

The fractional cavity volume is the fraction of void space occupied by spherical cavities defined by CESA.[14] In other words, not all of the free volume is in the form of well-defined spherical cavities. FCV is yet another measure of free volume. The average cavity size $\langle x \rangle$ is calculated as follows:

$$\langle x \rangle = \frac{\int_0^\infty x^3 P(v)dx}{\int_0^\infty x^2 P(v)dx} \qquad (11)$$

where x is the cavity size, and $P(v)$ is the volume distribution obtained from CESA.

Experimental permeation coefficients for oxygen are also included in Table 2. The FFV, FCV, and the average cavity size of PTMSP are the highest among these three polymers. The FFV, FCV, and the average cavity size of PTMSDPA are larger than those of PDPA, which correlate with the higher permeability in PTMSDPA than in PDPA.

5.2. Cavity Size Distribution. The cavity size distributions of PTMSDPA and PDPA determined using CESA are presented in Figures 4 and 5. The distribution in Figure 4 is shifted to larger cavity sizes relative to that of PDPA. To quantitatively compare the cavity size distributions of PTMSDPA and PDPA, the cumulative distributions of the two polymers are shown in Figure 6. The cumulative distribution for PTMSDPA is shifted toward larger cavity sizes. In PDPA, 50% of the cavities exceed 4.9 Å, whereas 50% of the cavities in PTMSDPA exceed 7.6 Å. Although cavity size distribution of polymeric materials can be probed by positron annihilation lifetime spectroscopy (PALS), there are no PALS data available for PTMSDPA and PDPA yet.
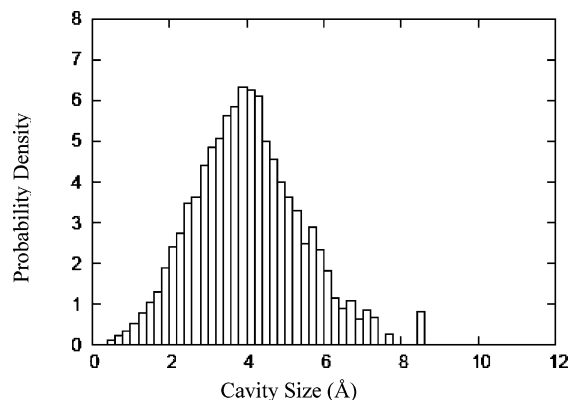

Figure 5. Cavity size distribution in PDPA at $T = 298$ K and $\rho = 1.04$ g/cm^3 from molecular simulation. The average cavity size is 5.0 Å, and the fractional cavity volume is 10.8%. PDPA has a higher fraction of smaller cavities than PTMSDPA.
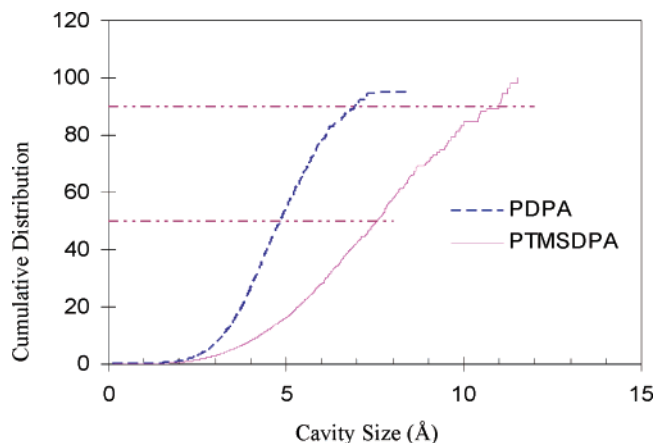

Figure 6. Comparison of cumulative cavity size distributions in PTMSDPA and PDPA

5.3. Diffusivity of CO$_2$ in PTMSDPA and PDPA. The diffusivity of CO$_2$ in PTMSDPA and PDPA was calculated by eq 8. CO$_2$ diffuses faster in PTMSDPA than PDPA, which may be due to the larger cavities in PTMSDPA. The diffusion coefficients obtained from molecular dynamics simulations are recorded in Table 3 along with the experimental data. We observe very good agreement between the simulations and experiments. The diffusion coefficient of CO$_2$ in PTMSP is the highest among all three polymers.
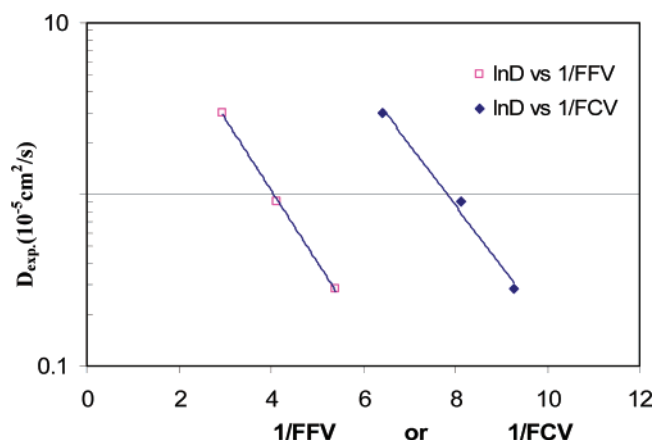
5.4. Solubility and Permeability of CO$_2$ in PTMSDPA and PDPA. Table 3 presents the simulation results for diffusivity, solubility and permeability of CO$_2$ in PTMSP, PTMSDPA, and PDPA and the corresponding experimental data. The solubility of CO$_2$ in PTMSP and PTMSDPA is measured using the Widom insertion method. The simulation solubility of CO$_2$ in PTMSP compares quite well to the experimentally measured solubility. However, the simulation predicts a much higher solubility of CO$_2$ in PTMSDPA than is observed experimentally. The large error in the CO$_2$ solubility in PTMSDPA may be due to the large error in the calculation of Coulombic interaction energy. The error in the CO$_2$ solubility in PDPA is so large that the simulated value is not acceptable anymore.

With simulation based values for the solubility and diffusion coefficients, we can use eq 2 to estimate the permeability of CO$_2$ in each polymer. The permeability predicted by simulation compares well with the experimental permeability for PTMSP. The simulation results overpredict the experimental results for PTMSDPA. Nevertheless, the computer simulations

Simulation and Experimental Study of Polyacetylenes

J. Phys. Chem. B, Vol. 110, No. 25, 2006 **12671**

TABLE 3: Sorption and Transport Properties of CO_2 in PTMSP,[15] PTMSDPA and PDPA

polymer	solubility		diffusivity (10^{-5} cm^2/s)		permeability (barrers)	
	simulation	experiment	simulation	experiment	simulation	experiment
PTMSP[15]	10.7 ± 1.6	9.6	3.5 ± 0.05	3.0	35000	35200
PTMSDPA	13.9 ± 5.0	4.8	1.1 ± 0.08	0.9	19400	4600
PDPA	NA[a]	4.5	0.6 ± 0.07	0.28	NA	1300

[a] The error in the calculation of Coulombic interaction energy in CO_2 solubility in polymer PDPA is too large to report.
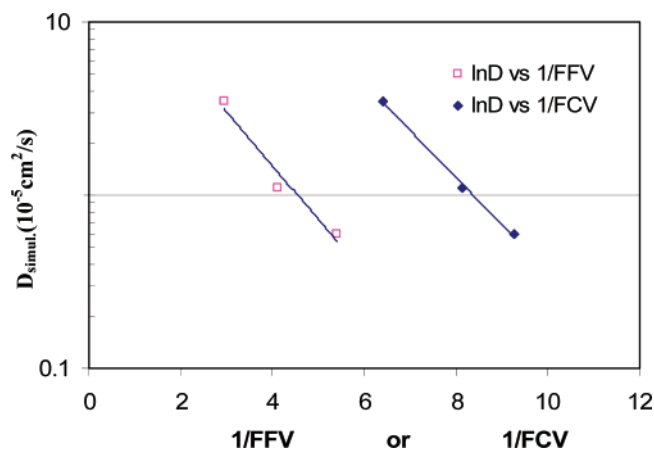
Figure 7. Plot of $\ln D_{simul.}$ vs 1/FFV and 1/FCV for the diffusion of CO_2 in three polymers.

Figure 8. Plot of $\ln D_{exp.}$ vs 1/FFV and 1/FCV for the diffusion of CO_2 in three polymers.

predict that the CO_2 permeability in PTMSP is higher than that in PTMSDPA, which is consistent with the experimental data.

5.5. Diffusivity and Free Volume. In Figure 7, we plot the 1/FCV and 1/FFV vs the simulated diffusion coefficients of CO_2 in three polymers. It shows that the diffusion coefficients have an exponential relationship with FFV (or FCV), which is consistent to the free volume theory:[30,31]

$$D = A \cdot \exp(-B/FFV) \qquad (4)$$

where A and B are constants. A slight change in FFV (or FCV) will lead to a relatively dramatic change in the diffusion coefficients. Takeuchi and Okazaki[32] have conducted molecular dynamics simulation of diffusion of simple gas molecules in a short chain polymer. They also found their simulated diffusion coefficients obeyed free volume theory very well. In Figure 8, we also plot the 1/FCV and 1/FFV vs the experimentally measured CO_2 diffusion coefficients in three polymers. The measured CO_2 diffusion coefficients also have an exponential relationship with FFV (or FCV).

6. Conclusions

Molecular modeling techniques have been applied to study cavity size distributions and transport properties of two recently synthesized substituted acetylene-based polymers, PTMSDPA and PDPA. Using atomistic models, cavity size (free volume) distributions determined by a combination of molecular dynamics and Monte Carlo methods are consistent with the observation that PTMSDPA is more permeable than PDPA. The average spherical cavity size in PTMSDPA is 7.5 Å, whereas it is only 5.0 Å in PDPA. The CO_2 diffusivity in these polymers was also obtained through both molecular simulation and experimental techniques. The diffusivity of CO_2 in PTMSDPA is higher than that in PDPA. Relatively good agreement is observed between the simulation and experimental data.

References and Notes

(1) Masuda, T.; Higashimura, T. *Adv. Polym. Sci.* **1987**, *81*, 121.
(2) Masuda, T.; Higashimura, T. *ACS Adv. Chem. Ser.* **1990**, *No. 224*, 641.
(3) Toy, L. G.; Nagai, K.; Freeman, B. D.; Pinnau, I.; He, Z.; Masuda, T.; Teraguchi, M.; Yampolskii, Y. P. *Macromolecules* **2000**, *33*, 2516−2524.
(4) Merkel, T. C.; Bondar, V.; Nagai, K.; Freeman, B. D. *J. Polym. Sci.: Part B: Polym. Phys.* **2000**, *38*, 273−296.
(5) Pinnau, I.; Casillas, C. G.; Morisato, A.; Freeman, B. D. *J. Polym. Sci.: Part B: Polym. Phys.* **1996**, *34*, 2613−2621.
(6) Nagai, K.; Nakagawa, T. *J. Membr. Sci.* **1995**, *105*, 261−272.
(7) Teraguchi, M.; Masuda, T. *Macromolecules* **2002**, *35*, 1149−1151.
(8) Raharjo, R. D.; Lee, H. J.; Freeman, B. D.; Masuda, T.; Sakaguchi, T. *Polymer* **2005**, *46*, 6316−6324.
(9) Shantarovich, V. P.; Kevdina, I. B.; Yampolskii, Y. P.; Alentiev, A. Y. *Macromolecules* **2000**, *33*, 7453−7466.
(10) Victor, J. G.; Torkelson, J. M. *Macromolecules* **1987**, *20*, 2241−2250.
(11) Sastry, S.; Truskett, T. M.; Debenedetti, P. G.; Torquato, S.; Stillinger, F. H. *Mol. Phys.* **1998**, *95*, 289.
(12) Arizzi, S.; Mott, P. H.; Suter, W. *J. Polym. Sci.: Part B: Polym. Phys.* **1992**; *30*, 415.
(13) in 't Veld, P. J.; Stone, M. T.; Truskett, T. M.; Sanchez, I. C. *J. Phys. Chem. B* **2000**, *104*, 12028−12034.
(14) Wang, X. Y.; Lee, K. M.; Lu, Y.; Stone, M. T.; Sanchez, I. C.; Freeman, B. D. *Polymer* **2004**, *45*, 3907−3912.
(15) Wang, X. Y.; Lee, K. M.; Lu, Y.; Stone, M. T.; Sanchez, I. C.; Freeman, B. D. In *New Polymeric Materials,* ACS Symposium Series 916; Korugic-Karasz, L. S., MacKnight, W. J., Martuscelli, E., Eds.; American Chemical Society: Washington, DC, 2005.
(16) Wang, X. Y.; in 't Veld, P. J.; Lu, Y.; Sanchez, I. C.; Freeman, B. D. *Polymer* **2005**, *46*, 9155−9161.
(17) Nakagawa, T. In *Polymeric Gas separation Membranes*, 1st ed.; Paul, D. R., Yampol'skii, Y. P. Eds.; CRC: Boca Raton, FL, 1994; p 155.
(18) Kestinn, R. E.; Fritzsche, A. K. *Polymeric Gas separation Membranes*, Wiley-Interscience Publication: New York, 1993.
(19) Frenkel, D.; Smit, B. *Understanding Molecular Simulation*, 2nd ed.; Academic Press: New York, 1996
(20) Stone, M. T.; in 't Veld, P. J.; Lu, Y.; Sanchez, I. C. *Mol. Phys.* **2002**, *100*, 2773−2782.

(21) Sanchez, I. C.; Rodgers, P. A. *Pure Appl. Chem.* **1990**, *62*, 2107−2114.

(22) Rodgers, P. A.; Sanchez, I. C. *J. Polym. Sci., Part B: Polym. Phys.* **1993**, *31*, 273−277.

(23) Materials Studio is a package developed by Accelrys Inc., http://www.accelrys.com/, San Diego, CA, 2002.

(24) Sun, H. *J. Phys. Chem. B* **1998**, *102*, 7338−7364.

(25) Charati, S. G.; Stern, S. A. *Macromolecules* **1998**, *31*, 5529−5535.

(26) Stern, S. A.; Gareis, P. J.; Sinclair, T. F.; Mohr, P. H. *J. Appl. Polym. Sci.* **1963**, *7*, 2035−2051.

(27) Koros, W. J.; Paul, D. R.; Rocha, A. A. *J. Polym. Sci., Part B: Polym. Phys.* **1976**, *14*, 687−702.

(28) van Krevelen, W. D. *Properties of Polymers*, 3rd ed.; Elsevier: Amsterdam, 1997; p71.

(29) Sanchez, I. C.; Cho, J. *Polymer* **1995**, *36*, 2929−2939.

(30) Cohen, M. H.; Turnbull, D. J. *J. Chem. Phys.* **1959**, *31*, 1164−1169.

(31) Thran, A.; Kroll, G.; Faupel, F. *J. Polym. Sci., Part B: Polym. Phys.* **1999**, *37*, 3344−3358.

(32) Takeuchi H, Okazaki K. *J. Chem. Phys.* **1990**, *92*, 5643−5652.